JCTC Journal of Chemical Theory and Computation

Article

pubs.acs.org/JCTC

A Full Dimensionality Approach to Evaluate the Nonlinear Optical Properties of Molecules with Large Amplitude Anharmonic Tunneling Motions

Marc Garcia-Borràs,[†] Miquel Solà,[†] David Lauvergnat,[‡] Heribert Reis,*[,§] Josep M. Luis,*[,†] and Bernard Kirtman[∥]

[†]Institut de Química Computacional and Departament de Química, Universitat de Girona, Campus Montilivi, 17071 Girona, Catalonia, Spain

[‡]Laboratoire de Chimie Physique, CNRS, Bât. 349, UMR 8000, Orsay F-91405, France and Université Paris-Sud, Orsay F-91405, France

[§]Institute of Biology, Medicinal Chemistry and Biotechnology, National Hellenic Research Foundation, 48 Vas. Constantinou Ave., Athens 116 35, Greece

[∥]Department of Chemistry and Biochemistry, University of California, Santa Barbara, California 93106, United States

Supporting Information

ABSTRACT: Previously, a reduced dimensionality approach was used to determine the vibrational contribution to nonlinear optical properties for molecules with large amplitude anharmonic modes that takes into account tunneling between potential wells (Luis, J. M.; Reis, H.; Papadopoulos, M. G.; Kirtman, B. *J. Chem. Phys.* **2009**, *131*, 034116). Here, the treatment is extended, again using ammonia as an example, to include the remaining modes at several approximate levels. It is shown that this extension is essential to obtaining the correct results. Our new approach fully accounts for tunneling and avoids possible convergence problems associated with the normal coordinate expansion of the potential energy surface in a single-well treatment. For accurate numerical values, a good treatment of electron correlation is required along with a flexible basis set including diffuse functions.

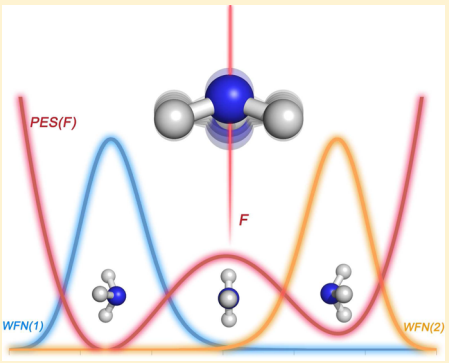

1. INTRODUCTION

The nonlinear (and linear) response of chemical systems to dynamic and/or static electric fields continues to be a subject of keen interest from both a theoretical and practical perspective.[1] It is now well-known that the (non-) linear response properties, i.e., the (hyper)polarizabilities or electric susceptibilities, depend importantly on the nuclear as well as the electronic motions.[2] Indeed, the vibrational contribution associated with nuclear motions can often be similar in magnitude to, or even exceed, the pure electronic contribution. A perturbation treatment of the former, valid for nonresonant processes, was presented by Bishop and Kirtman (BKPT) about 20 years ago and is still extensively employed.[3] However, BKPT is based on a double harmonic (mechanical and electrical) initial approximation, and when there are large amplitude anharmonic modes, that treatment may be either slowly convergent or nonconvergent. A paradigmatic case for which nonconvergence is expected is a molecule with equivalent minima separated by sufficiently low barriers[2d] such that tunneling is important, but there are many other examples.[4] Moreover, even when the anharmonicity can be treated perturbatively, the BKPT calculations can be quite time-consuming for large systems. As a result, other approaches have been, and continue to be, pursued.

One alternative is the nuclear relaxation (NR) approach developed by some of us and collaborators, which is based on the change in equilibrium geometry induced by a static electric field.[5] Thus, although related to BKPT (see further below), this approach is variational rather than perturbative. A particular variant is the so-called finite field nuclear relaxation (FF-NR) method. In the FF-NR method, the electronic energy and electric dipole properties are calculated at the field-dependent equilibrium geometry. Then, each of these properties is expanded as a power series in the field, and the resulting coefficients yield the static vibrational (hyper)polarizabilities, as well as the infinite optical frequency approximation (IOFA) for the *dynamic* vibrational hyperpolarizabilities corresponding to most major nonlinear optical processes. It can be shown that the static vibrational (hyper)polarizabilities so obtained contain a well-defined set of the leading terms in the BKPT formulas. The same is true of the *dynamic* properties which, within the IOFA, require that $(\omega_\nu/\omega_{opt})^2 \ll 1$ for all external field optical

Received: September 14, 2012
Published: October 25, 2012

   dx.doi.org/10.1021/ct300805p | *J. Chem. Theory Comput.* 2013, 9, 520−532

frequencies (ω_{opt}) and all vibrational frequencies (ω_ν) of the system under investigation. Numerical studies show, as expected, that the IOFA is quite accurate for all field frequencies that lie substantially above the infrared region.[6] There are variants of the FF-NR procedure that allow the region of applicability to be extended to lower optical frequencies[7] and also permit most, or all, of the computations to be carried out analytically.[6c,8]

The FF-NR method can be extended by adding the zero-point vibrational average (zpva) to the pure electronic energy and electric dipole properties (all computed at the field-dependent equilibrium geometry) prior to the power series expansion in the field.[5c] Then, higher-order anharmonicity contributions will be included. In principle, the zpva can be evaluated using perturbation theory order-by-order, which would add successively higher-order perturbation theory terms to the calculated vibrational (hyper)polarizabilities. Alternatively, one can compute the entire zpva variationally, in which case the complete vibrational (hyper)polarizabilities would be obtained, thereby avoiding the problem of a possible slow or nonconvergent perturbation treatment.[2d,9] Except for very small molecules, approximations are inevitably introduced in calculating the entire zpva. These approximations could, of course, introduce other convergence problems. However, one may also attempt to avoid such problems as in the treatment presented here.

As a brief aside, we mention that a response theory formalism for computing vibrational nonlinear optical properties has recently been presented by Christiansen and co-workers.[10] Their formalism includes a term that is missing in the BKPT due to the assumption that, in the nonresonant regime, electronic transition frequencies are much larger than the external laser optical frequencies. Nevertheless, for static and IOFA dynamic properties, which are the only cases considered in this paper, the missing terms vanish.[11]

In the first attempt at a treatment of vibrational contributions with the full zpva, some of us and collaborators combined the FF-NR procedure with the vibrational self-consistent field (VSCF) and vibrational second-order Møller−Plesset perturbation theory (VMP2) methods.[9a] For benchmark purposes, a full vibrational (FVCI) treatment was also carried out.[9a] However, to make the FVCI calculations feasible, the potential energy surfaces (PESs) had to be truncated after the quartic terms in a full $3N - 6$ dimensional normal coordinate power series expansion. Static vibrational (hyper)polarizabilities were, then, computed for H_2O, HOOH, and HSSH. As expected, the results confirmed that BKPT is not reliable for HOOH and HSSH, which have large amplitude anharmonic torsional modes. Furthermore, it was shown that VMP2 is insufficient for these molecules; one must choose a higher-level method such as vibrational coupled cluster (VCC) or VCI.

Subsequently, Christiansen's direct FVCI treatment was combined with our FF-NR approach and applied, with 6D quartic and sextic normal mode expansions of the PES,[9b] and the IOFA dynamic vibrational (hyper)polarizabilities were determined using normal coordinate power series expansions for the electric dipole property surfaces. Again, good results were obtained for H_2O, but the power series expansion for the NH_3 PES, based on displacements from a single well of the double minimum inversion potential, were seemingly nonconvergent. The nonconvergent behavior was found to be associated with the large amplitude anharmonic inversion (or umbrella) mode. Thus, in a following work, the umbrella mode of NH_3 was, instead, treated "exactly" by means of a simple reduced one-dimensional (1D) calculation using an appropriate curvilinear coordinate.[2d] The vibrational kinetic energy operator, then, does not have a simple quadratic form. In order to get around that difficulty, we used the numerical, but exact, procedure implemented in the TNUM code to obtain the appropriate operator.[12] The coupling to all other modes was included approximately by optimizing the geometry at each point along the 1D PES but was otherwise ignored (as was the smaller contribution of the remaining, i.e., inactive, modes). On the basis of the reduced 1D calculations, the problematic nature of the single well PES was identified (incorrectly as it now turns out).

Although the reduced 1D treatment avoids the nonconvergence problem, it may not adequately account for the other modes. Hence, the purpose of the current study is to extend our treatment to fully include all $3N - 6$ vibrational degrees of freedom. As noted above, in our previous work,[2d] the numerical TNUM code was used to calculate the kinetic energy operator for the inversion mode. Such a numerical procedure is advantageous, in general, since it can be applied universally for all modes as opposed to an analytical formulation. Thus, we retain this treatment of the kinetic energy operator and combine it with the full potential for the active modes (limited in number) plus an approximate quadratic potential for all the remaining (inactive) modes. To properly include the coupling with active modes the coefficients of the quadratic terms need to depend on the instantaneous positions of the active degrees of freedom. This procedure leads to the harmonic adiabatic approximation (HADA) and to the coupled harmonic adiabatic channels (cHAC) model, both implemented in Lauvergnat's ELVIBROT code.[13]

The computational methods and details that are employed in the current paper are described in the following section. In the section after that, we present results obtained for ammonia. This molecule was chosen because it is known to provide an excellent test case from previous work. Most importantly, it turns out that ammonia very nicely illustrates how the neglect of coupling between active and inactive coordinates can lead to spurious conclusions.

2. COMPUTATIONAL METHODS

A. Quantum Nuclear Models. The development of general quantum dynamics programs has made much progress recently, as nicely discussed in a recent review.[14] Nowadays, there are several general codes, which lift previous limitations on the number of atoms or coordinates that can be employed. In most of these programs,[15] rectilinear normal modes are used. However, when large amplitude motions and/or several minima are important, the calculations are more efficient using curvilinear coordinates. Unfortunately, the selection of these coordinates is difficult to automate, because it depends strongly on the process under study. There are, furthermore, other aspects that make automation problematic. The representation of the PES is one of the most difficult. Direct point by point evaluation of the PES, like the n-mode representation used in most VSCF programs,[15b−d] is one way to solve this problem. However, that approach is time-consuming, especially if one needs an accurate description of the vibrational states, and therefore and a high-level quantum chemistry treatment.

Despite the difficulties involved, several general codes based on curvilinear coordinates have been developed: GENIUSH,[16]

TROVE,[17] MrPropa,[18] PVSCF,[19] ElVibRot,[13] and others. In all of them, the kinetic energy operator (KEO) is computed through a numerical approach as in Tnum.[12] The MCTDH code[20] should also be mentioned here. Like the above, it has been used to study large and floppy systems,[21] but the KEO analytical expression must be given.

The present study using ElVibRot employs models based on a separation between the active coordinates, $\mathbf{q}_{act}$, and the inactive ones, $\mathbf{q}_{inact}$, of a molecular system containing N atoms. Selection of the n active coordinates and m inactive ones is based, as usual, on the chemical or physical process studied. There are several models[13] with an increasing accuracy that could be used:

i. *Reduced dimensionality or constrained models* (rigid[22] or flexible[23]), where the inactive coordinates are somehow neglected. This reduces the quantum problem to n active coordinates only. In rigid models, the inactive coordinates are frozen at the values of a reference geometry (energy minimum, transition state...), i.e. $\mathbf{q}_{inact} = \mathbf{q}_{ref}$, whereas in flexible models the inactive coordinates are functions of the active ones, $\mathbf{q}_{inact} = \mathbf{q}_{inact}^{opt}(\mathbf{q}_{act})$. The functional dependence can be obtained by an energy minimization of the inactive coordinates for fixed values of the active ones.

ii. *Harmonic adiabatic channels*:[24] The complete wave function is decomposed as a sum of products of an active and an inactive part:

$$\psi_{I,U}(\mathbf{q}_{act}, \mathbf{q}_{inact}) = \sum_{I,U} C_{I,U}\varphi_I(\mathbf{q}_{act})\chi_U(\mathbf{q}_{inact}; \mathbf{q}_{act}) \quad (1)$$

where the $\chi_U(\mathbf{q}_{inact};\mathbf{q}_{act})$ are eigenfunctions of an inactive Hamiltonian parametrized by the active coordinates. In our treatment, we use a harmonic Hamiltonian for displacements of the inactive coordinates about the minimum energy path. Thus, the total potential is expressed as

$$V(\mathbf{q}) = V_0(\mathbf{q}_{act}) + V_2(\mathbf{q}) + \mathcal{R}(\mathbf{q}) \quad (2)$$

with

$$V_2(\mathbf{q}) = \frac{1}{2}\sum_{k,l} h_{k,l}(\mathbf{q}_{act})(q_{inact}^{k} - q_{inact}^{opt,k}(\mathbf{q}_{act}))(q_{inact}^{l} - q_{inact}^{opt,l}(\mathbf{q}_{act})) \quad (3)$$

in which $h_{k,l}(\mathbf{q}_{act})$ and $q_{inact}^{opt,k}(\mathbf{q}_{act})$ are, respectively, the elements of the Hessian matrix and the optimal inactive coordinates for the active domain. $V_2(\mathbf{q})$ is the quadratic contribution associated with displacements of the inactive coordinates; there is no first order contribution because we are using a minimum energy path. $\mathcal{R}(\mathbf{q})$ is the remainder of the Taylor expansion (this term is ignored in the present study).

After integration over the inactive coordinates, the total Hamiltonian can be represented as a matrix $H_{U,W}(\mathbf{q}_{act},\partial_{q_{act}})$ containing the operators $\partial_{\mathbf{q}_{act}}$ that operate only on the active variables. Neglecting the matrix elements coupling different adiabatic channels (i.e., U not equal to W) leads to an effective nD Hamiltonian for each adiabatic state. This approximation is usually denoted as the $n + m$D ($n + m = 3N - 6$) harmonic adiabatic approximation (HADA). Retaining the off-diagonal matrix elements leads to the coupled harmonic adiabatic channels (cHAC) model. When the number of channels is large enough, the latter turns out to be equivalent to the exact solution (assuming $\mathcal{R}(\mathbf{q})$ can be ignored). The model just described is related to the adiabatic approximation,[25] the reaction path Hamiltonian,[26] the reaction surface Hamiltonian[27], and similar approaches.[28]

For all of the above models, the use of curvilinear active coordinates is essential to performing the quantum dynamics simulations efficiently. However, the resulting analytical expression of the kinetic energy operator (KEO) can be difficult to obtain. In order to overcome this problem, it is common to use numerical methods,[12,16,23a,29] a feature recognized for many years.[30] In Tnum, the KEO due to nuclear motion is expressed as ($J = 0$, i.e., rotational ground state):

$$\mathbf{T}(\mathbf{q}, \partial_{\mathbf{q}}) = \sum_{i\le j} f_2^{i,j}(\mathbf{q})\partial_{i,j}^2 + \sum_i f_1^i(\mathbf{q})\partial_i + V_{extra}(\mathbf{q})$$

$$dv = \rho(\mathbf{q})dq^1...dq^n \quad (4)$$

with the functions $f_2^{ij}(\mathbf{q})$, $f_1^i(\mathbf{q})$ and the extrapotential term,[31] $V_{extra}(\mathbf{q})$, determined on a multidimensional grid using the metric tensors obtained by evaluating the body-fixed frame (BF) Cartesian coordinates as a function of the curvilinear ones. The calculations are done *numerically*, but the procedure is *exact*. Primitive internal coordinates (which can be obtained from a Z-matrix for instance) are converted in Tnum to the desired curvilinear coordinates. Finally, the volume element, dv, is not necessarily Euclidean.[12]

B. Models for Ammonia. As already mentioned, the selection of coordinates is critical. Several different sets have been used for ammonia in the past.[24a,32] In the present study, we use the six symmetrized coordinates proposed by Handy et al. obtained by combining the unsymmetrized coordinates depicted in Figure 1.[32a] Thus, the inversion motion is described

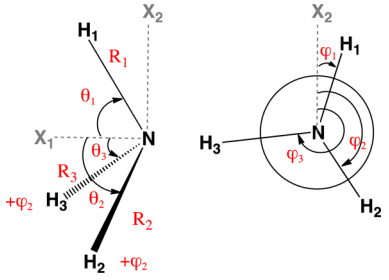

Figure 1. Unsymmetrized coordinates for ammonia.

by $\theta = 1/3(\theta_1 + \theta_2 + \theta_3)$, and the two degenerate scissor modes are described by the symmetrized linear combinations of the φ_i angles: $\varphi_{e1} = 1/\sqrt{2}(\varphi_2 - \varphi_3)$ and $\varphi_{e2} = 1/\sqrt{6}(2\varphi_1 - \varphi_2 - \varphi_3)$. Similarly, the symmetrized stretching modes are $R_a = 1/3(R_1 + R_2 + R_3)$, $R_{e1} = 1/\sqrt{2}(R_2 - R_3)$, and $R_{e2} = 1/\sqrt{6}(2R_1 - R_2 - R_3)$.

In the present study, we use two reduced dimensionality models: (i) a flexible 1D model with the inversion angle θ as the active coordinate—the symmetric stretch, R_a, is taken to be a function of θ while the other coordinates remain constant—(ii) a rigid 2D model with θ and R_a as the active coordinates. In order to take into account the inactive modes, we also use the HADA and cHAC treatments with either one or two active coordinates. This yields the models convention-

dx.doi.org/10.1021/ct300805p | J. Chem. Theory Comput. 2013, 9, 520−532

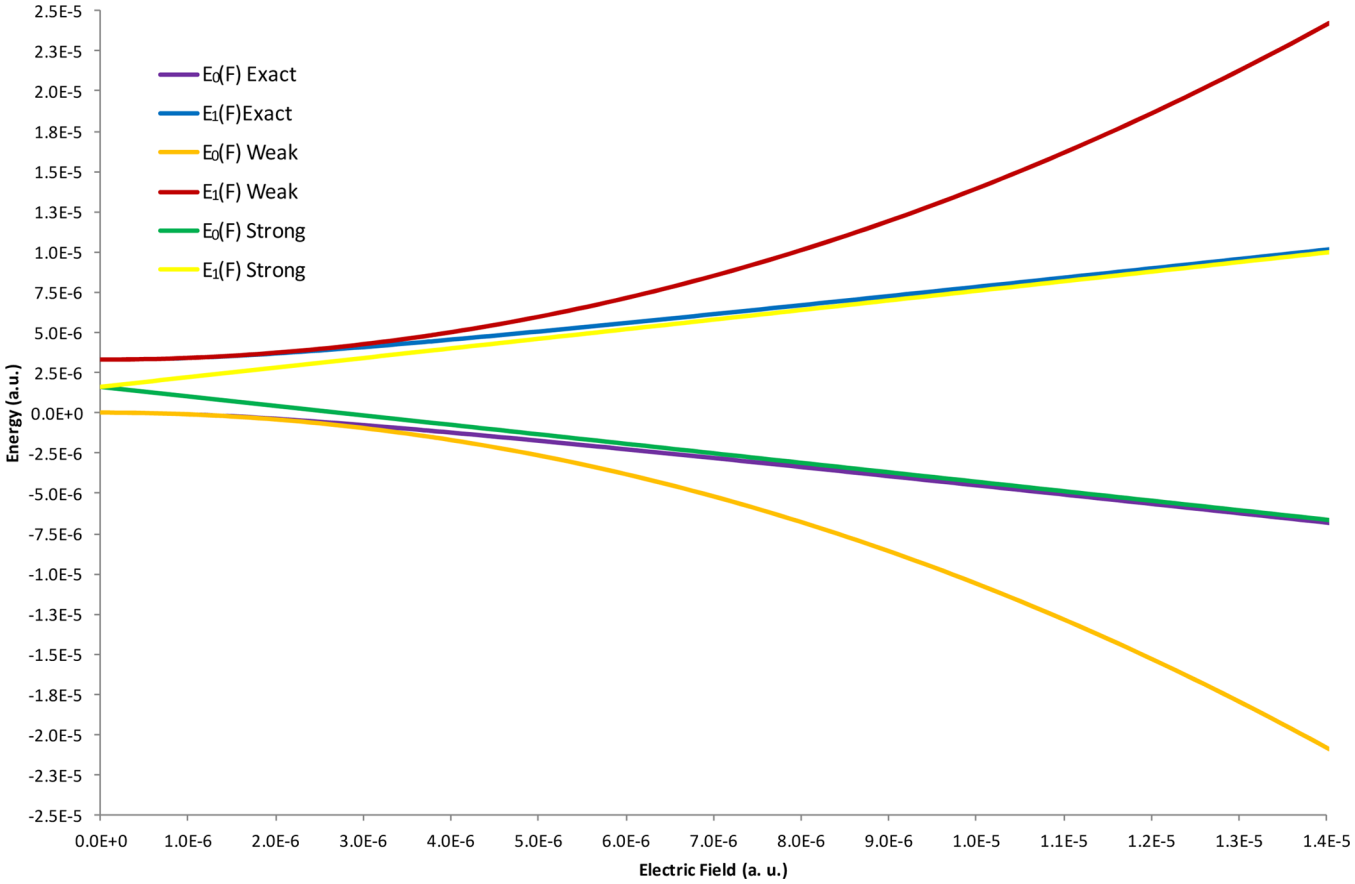

Figure 2. Field-dependent energy for the lowest pair of vibrational states of ammonia computed using the exact expression, the weak field approximation, and the strong field approximation.

ally labeled as 1+5D HADA, 1+5D cHAC, 2+4D HADA, and 2+4D cHAC. For those cases, the parameters of the Hamiltonian, $h_{k,l}(\mathbf{q}_{act})$ and $q_{inact}^{opt,k}(\mathbf{q}_{act})$, are fit to analytical expressions (polynomials). Due to symmetry, only the coordinate R_a has to be optimized as a function of the inversion angle θ (for the 1D model). For the Hessian, only four unique elements have to be determined, h_{R_a,R_a}, $h_{R_{e1},R_{e1}}$, $h_{\varphi_{e1},\varphi_{e1}}$, and $h_{R_{e1},\varphi_{e1}}$.

C. Evaluation of the (Hyper)Polarizabilities for a Molecule with Double Minimum Well Potential. In our previous work,[2d] the evaluation of vibrational (hyper)-polarizabilities was carried out for NH_3 using generalized Van Vleck quasidegenerate perturbation theory (GVV-PT) to take into account tunneling between equivalent potential wells for the lowest pair of vibrational states. Although NH_3 has inversion symmetry, it is worth noting that GVV-PT can be applied equally as well to nonequivalent minima. It also can be used when there are more than two minima and/or when it is desirable to include additional vibrational states in the model (or reference) space. Hence, the overall GVV-PT approach is quite general. It will be used here for all of our models.

For NH_3, the field-dependent GVV-PT Hamiltonian matrix for the two-dimensional reference space (lowest pair of vibrational states) takes the general form (through fourth-order in the field):

$$\hat{H}(F_z) = \begin{pmatrix} E^+(0) - \frac{1}{2}\alpha_{zz}^+ F_z^2 - \frac{1}{24}\gamma_{zzzz}^+ F_z^4 & -\mu_z^\pm F_z - \frac{1}{6}\beta_{zzz}^\pm F_z^3 \\ -\mu_z^\pm F_z - \frac{1}{6}\beta_{zzz}^\pm F_z^3 & E^-(0) - \frac{1}{2}\alpha_{zz}^- F_z^2 - \frac{1}{24}\gamma_{zzzz}^- F_z^4 \end{pmatrix} \quad (5)$$

where the superscript + (−) indicates the symmetric (antisymmetric) reference state and F_z is an electric field along the 3-fold symmetry axis (z). Due to symmetry, the matrix elements on the diagonal are even order in the field, whereas the off-diagonal terms are odd order. By using the "exact" field-dependent vibrational wave functions in computing these matrix elements (see below), the coupling to other vibrational states is implicitly removed. All pure vibrational (J = 0) contributions, including the zpva, are contained in the matrix elements.

Finally, in GVV-PT, the field-dependent energies are obtained by solving the secular equation associated with the Hamiltonian matrix in eq 5. In general, these energies cannot be written as a power series in the field, and comparison with the experiment must be made for each individual field. There are two limiting cases, however, for which one can obtain a

dx.doi.org/10.1021/ct300805p | J. Chem. Theory Comput. 2013, 9, 520−532

power series expansion in terms of the field (see further below): either $|E^+(0) - E^-(0)|$ is much greater than $|2\mu_z^{\pm} F_z|$ (i.e., weak field approximation) or vice versa (strong field approximation). Of course, the coefficients in the expansion, i.e., the (non)linear optical properties, will be different in the two cases. This can readily be seen in Figure 2 where the exact field-dependent energies and the energies obtained with the strong and weak field approximations are represented. For fields smaller than 2.5×10^{-6} au (1.3×10^6 V/m), the field-dependent energies obtained with the weak field approximation reproduce very well the exact energies. On the contrary, for fields greater than 1.0×10^{-5} au (5.1×10^6 V/m), the field-dependent energies obtained with the strong field approximation match the exact results, whereas the energies obtained with the weak field approximation give much too large absolute values. Naturally, in the intermediate region, there is a crossover from one case to the other so that both power series expansions become invalid. For fields greater than |0.0004| au (the minimum field used here), NH_3 lies well within the strong field regime.

In Figure 3, we illustrate how the vibrational wave functions for the two lowest states of ammonia are altered when a static

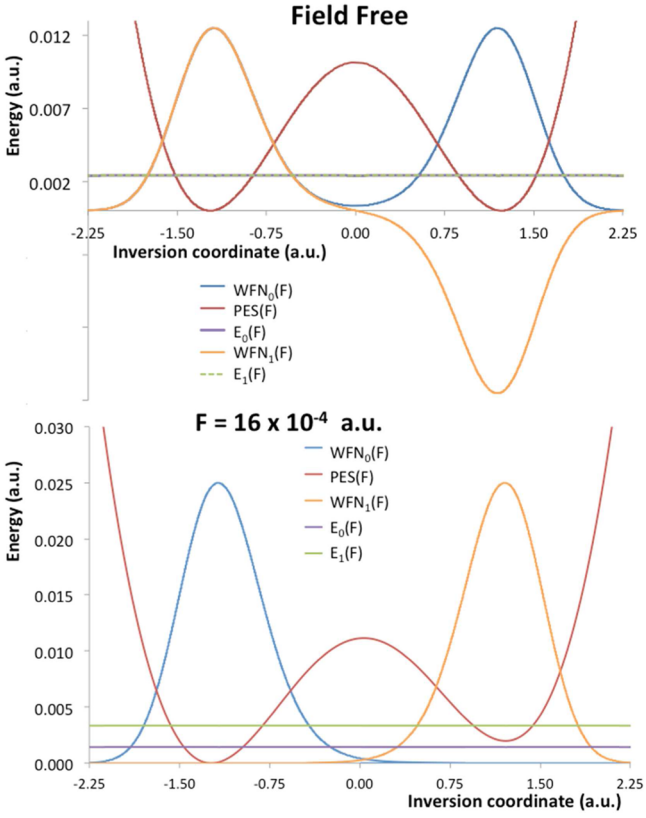

Figure 3. Inversion coordinate potential energy profile and vibrational wave functions and energies for the two lowest states of ammonia for the field free and $F_z = 16 \times 10^{-4}$ au cases.

external electric field is applied along the C_{3v} symmetry axis. In the field-free case, the probability of finding ammonia in either of the two wells is the same for both the symmetric and antisymmetric vibrational states. On the contrary, for an external electric field of 16×10^{-4} au, the ground state is completely localized in what has become the deeper well while the first excited state is localized in the other well.

The analytical expressions for the two lowest field-dependent vibrational energies obtained within the strong field approximation are given by[2d]

$$E_0(F) = E(0) - \mu_z F_z - \frac{1}{2}\alpha_{zz}F_z^2 - \frac{1}{6}\beta_{zzz}F_z^3 - \frac{1}{24}\gamma_{zzzz}F_z^4 \tag{6}$$

$$E_1(F) = E(0) + \mu_z F_z - \frac{1}{2}\alpha_{zz}F_z^2 + \frac{1}{6}\beta_{zzz}F_z^3 - \frac{1}{24}\gamma_{zzzz}F_z^4 \tag{7}$$

where $E(0) = 1/2[E^+(0) + E^-(0)]$, $\alpha_{zz} = 1/2[\alpha_{zz}^+ + \alpha_{zz}^-]$, $\gamma_{zzzz} = 1/2[\gamma_{zzzz}^+ + \gamma_{zzzz}^-]$, $\mu_z = \mu_z^{\pm}$, and $\beta_{zzz} = \beta_{zzz}^{\pm}$. For positive μ_z, $E_0(F)$ and $E_1(F)$ correspond to the ground and first excited states, respectively. From eqs 6 and 7, it is straightforward to derive formulas for the numerical field derivatives from which the diagonal z component of static dipole moment and vibrational (hyper)polarizabilities are obtained:

$$\mu_z = \frac{-E_1(2F_z) + E_0(2F_z) + 8E_1(F_z) - 8E_0(F_z)}{12F_z} \tag{8}$$

$$\alpha_{zz}(0;0) = [E_1(4F_z) + E_0(4F_z) - 17E_1(2F_z) - 17E_0(2F_z) + 16E_1(F_z) + 16E_0(F_z)]/[36F_z^2] \tag{9}$$

$$\beta_{zzz}(0;0,0) = \frac{E_1(2F_z) - E_0(2F_z) - 2E_1(F_z) + 2E_0(F_z)}{2F_z^3} \tag{10}$$

$$\gamma_{zzzz}(0;0,0,0) = [-E_1(4F_z) - E_0(4F_z) + 5E_1(2F_z) + 5E_0(2F_z) - 4E_1(F_z) - 4E_0(F_z)]/[15F_z^4] \tag{11}$$

The above static (hyper)polarizabilities include the electronic contribution and all vibrational contributions within the quantum nuclear model used. $E_0(F)$ and $E_1(F)$ are calculated variationally using the ElVibRot code for different electric field values. Exactly the same numerical values for the (hyper)-polarizabilities can be obtained from derivatives of the dipole moment rather than the energy. Here we have computed these properties using both sets of expressions (i.e., energy and dipole moment) in order to cross-check our results.

The properties obtained from eqs 8−11 may be written as a sum of four contributions: the electronic contribution, P^e; the nuclear relaxation contribution, P^{nr}; the zero-point vibrational average, P^{zpva}; and the remaining higher-order pure vibrational terms not included in P^{nr} denoted as P^{c-zpva} ($P = P^e + P^{nr} + P^{zpva} + P^{c-zpva}$). For μ, P^{nr} (and P^{c-zpva}) vanishes. For the other properties, P^{nr} can be easily computed using the standard NR approach.[5] The P^{zpva} term is determined here as the expectation value of $P^e(\mathbf{q}_{act})$ using the vibrational wave functions given by the quantum nuclear model. For the dipole moment, this value was compared with the result obtained from eq 8 to make sure that the two agree. Finally, the P^{c-zpva} contribution was determined as the difference between the total property value and the sum of the other three contributions.

By combining the field-dependent zero-point vibrationally averaged properties calculated using the ElVibRot code[13] with the FF-NR procedure, we have also obtained the IOFA *dynamic* (hyper)polarizabilities through the following expressions (see ref 2d):

dx.doi.org/10.1021/ct300805p | J. Chem. Theory Comput. 2013, 9, 520−532

Table 1. Ammonia Equilibrium Geometry (N−H Bond Distance, r_{N-H}, and H−N−H angle, θ_{H-N-H}) and Inversion Barrier Computed at Different *ab Initio* Levels[a]

	inversion barrier (cm^{-1})	abs. error[b] (inversion barrier)	r_{N-H} (Å)	abs. error[c] (r_{N-H})	θ_{H-N-H} (deg)	abs. error[c] (θ_{H-N-H})
experimental	1884.70		1.0116		106.68	
MP2/POL	2232.37	347.67	1.0238	0.0122	105.28	1.41
MP2/ATZ	1766.76	117.94	1.0118	0.0002	106.82	0.14
CCSD/ATZ	1894.11	9.41	1.0121	0.0005	106.70	0.02
CCSD/ACTZ	1844.56	40.14	1.0109	0.0007	106.83	0.14
CCSD(T)/ATZ	1933.82	49.12	1.0146	0.0030	106.50	0.18
CCSD(T)/ACTZ	1883.58	1.12	1.0134	0.0018	106.62	0.06
CCSD(T)/AQZ	1871.43	13.27	1.0128	0.0012	106.60	0.09

[a]The absolute errors with respect to experimental data are also given. [b]Experimental data taken from ref 40a. [c]Experimental data taken from ref 40b.

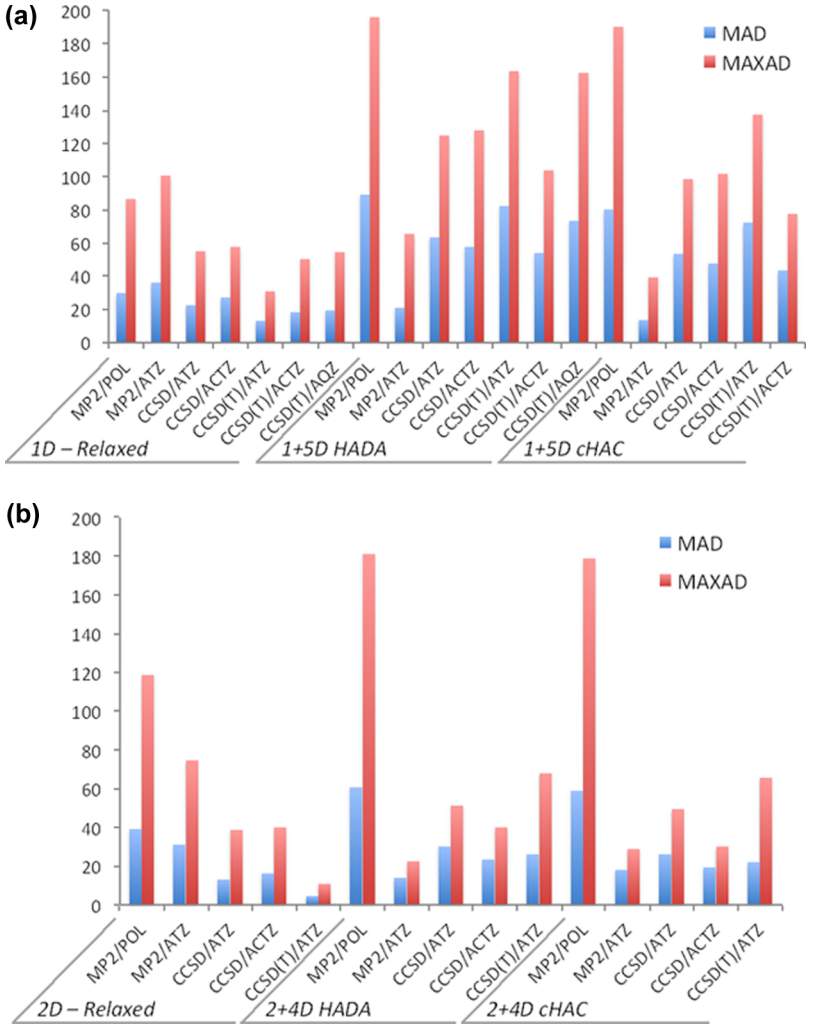

Figure 4. MAD and MAXAD, with respect to experimental data,[41] for the computed excitation energies of the first seven excited states of the ammonia umbrella mode. These calculations were done using several electronic structure levels for the PES and 1D relaxed, 1+5D HADA, and 1+5D cHAC (a) and 2D rigid, 2+4D HADA, and 2+4D cHAC (b) quantum nuclear models. All quantities are in cm^{-1}.

$$\beta^{e}_{zzz}(0;0,0) + \beta^{zpva}_{zzz}(0;0,0) + \beta^{nr}_{zzz}(-\omega;\omega,0)_{\omega\to\infty} + \beta^{c-zpva}_{zzz}(-\omega;\omega,0)_{\omega\to\infty} = \frac{-\alpha_{zz,1}(2F_z) + \alpha_{zz,0}(2F_z) + 8\alpha_{zz,1}(F_z) - 8\alpha_{zz,0}(F_z)}{12F_z} \quad (12)$$

$$\gamma^{e}_{zzzz}(0;0,0,0) + \gamma^{zpva}_{zzzz}(0;0,0,0) + \gamma^{nr}_{zzzz}(-\omega;\omega,0,0)_{\omega\to\infty} + \gamma^{c-zpva}_{zzzz}(-\omega;\omega,0,0)_{\omega\to\infty} = [\alpha_{zz,1}(4F_z) + \alpha_{zz,0}(4F_z) - 17\alpha_{zz,1}(2F_z) - 17\alpha_{zz,0}(2F_z) + 16\alpha_{zz,1}(F_z) + 16\alpha_{zz,0}(F_z)]/[36F_z^2] \quad (13)$$

dx.doi.org/10.1021/ct300805p | J. Chem. Theory Comput. 2013, 9, 520−532

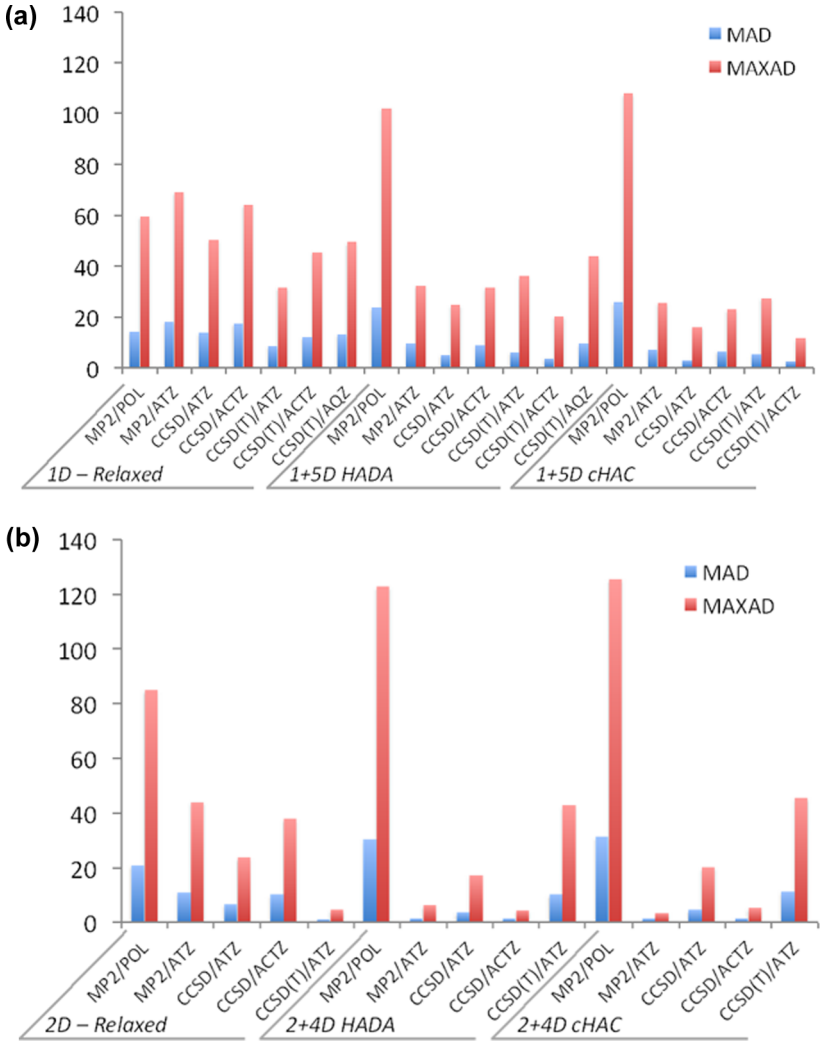

Figure 5. MAD and MAXAD, with respect to experimental data,[41] for the energy splitting due to inversion in the ground state, as well as in the three lowest excited states of the umbrella mode in ammonia. These computations were done using several electronic structure levels for the PES and 1D relaxed, 1+5D HADA, and 1+5D cHAC (a) and 2D rigid, 2+4D HADA, and 2+4D cHAC (b) quantum nuclear models. All quantities are in cm^{-1}.

$$\gamma^{e}_{zzzz}(0;0,0,0) + \gamma^{zpva}_{zzzz}(0;0,0,0) + \gamma^{nr}_{zzzz}(-2\omega;\omega,\omega,0)_{\omega\to\infty} + \gamma^{c-zpva}_{zzzz}(-2\omega;\omega,\omega,0)_{\omega\to\infty} = \frac{-\beta_{zzz,1}(2F_z) + \beta_{zzz,0}(2F_z) + 8\beta_{zzz,1}(F_z) - 8\beta_{zzz,0}(F_z)}{12F_z} \quad (14)$$

where $\alpha_{zz,0}(F_z)$ and $\alpha_{zz,1}(F_z)$ ($\beta_{zzz,0}(F_z)$ and $\beta_{zzz,1}(F_z)$) are the field-dependent static polarizability (first hyperpolarizability) for the ground and first excited vibrational states. As indicated above, the quantities $\beta^{nr}_{zzz}(-\omega;\omega,0)_{\omega\to\infty}$, $\gamma^{nr}_{zzzz}(-\omega;\omega,0,0)_{\omega\to\infty}$, and $\gamma^{nr}_{zzzz}(-2\omega;\omega,\omega,0)_{\omega\to\infty}$ were calculated by means of the standard FF-NR method,[5a] and then, eqs 12−14 yield the c-zpva contributions.

3. RESULTS AND DISCUSSION

The main goal of this paper is to extend previous calculations of the vibrational NLO properties of NH_3 so that all vibrations are included (although the so-called inactive modes are treated only quadratically along the active coordinates) and, in addition, tunneling between the two equivalent wells is fully taken into account. A necessary first step was to explore the accuracy of different *ab initio* electronic structure treatments for determining the PES, particularly with regard to the description of the vibrational energy levels for the umbrella motion of ammonia. We have used the MP2,[33] CCSD,[34] and CCSD(T)[35] *ab initio* methods together with several basis sets including the POL basis set developed by Sadlej,[36] and the correlation-consistent basis sets aug-cc-pVTZ (ATZ),[37] aug-cc-pVQZ (AQZ),[37] and aug-cc-pCVTZ (ACTZ).[37a,38] In all calculations with the ACTZ basis set, correlation of the nitrogen 1s electrons is taken into account. Each of these correlation-consistent basis sets contains diffuse functions in line with the results of Halonen and co-workers, who showed that this yields a large improvement in the calculated inversion barrier.[32b] All electronic structure and property calculations were performed using the Gaussian 09 suite of programs.[39]

In Table 1, we compare our MP2, CCSD, and CCSD(T) results for the ammonia equilibrium geometry and inversion energy barrier with experimental data.[40] At the MP2 level, the ATZ basis set clearly improves the description of both the inversion barrier and the equilibrium geometry given by the POL basis set. That is not surprising since the latter was designed for NLO properties rather than structure. For instance, with MP2/ATZ, the absolute error in the inversion

Table 2. Electronic and Vibrational Contributions to the Dipole Moment and to the Diagonal Component of the Static Linear Polarizability, As Well As the Static and IOFA Dynamic First Hyperpolarizabilities, along the C_3 Symmetry Axis[a]

	6D normal modes		1D		ElVibRot					
	fourth-order[b,d]	sixth-order[b,e]	$\theta^{c,f}$	$z^{c,g}$	1D relax.	1+5D HADA	1+5D cHAC	2D	2+4D HADA	2+4D cHAC
μ^{e}	−0.6209									
μ^{ZPVA}	0.0196	0.0180	0.0277	0.0303	0.0268	0.0200	0.0197	0.0244	0.0231	0.0229
μ	−0.6013	−0.6029	−0.5932	−0.5906	−0.5941	−0.6009	−0.6012	−0.5965	−0.5978	−0.5980
α_{zz}^{e} (0;0)	15.80									
α_{zz}^{nr} (0;0)	2.75									
α_{zz}^{ZPVA} (0;0)	0.46	0.46	0.13	0.15	0.13	0.09	0.09	0.22	0.43	0.43
α_{zz}^{c-ZPVA} (0;0)	0.88	0.63	1.05	1.12	1.05	0.64	0.64	0.86	0.57	0.56
α_{zz} (0;0)	19.89	19.64	19.73	19.82	19.73	19.28	19.28	19.63	19.55	19.54
β_{zzz}^{e} (0;0,0)	31.1									
β_{zzz}^{nr} (0;0,0)	115.1									
β_{zzz}^{ZPVA} (0;0,0)	0.0	0.0	−0.8	−0.8	−0.8	−0.8	−0.8	−0.6	0.2	0.2
β_{zzz}^{c-ZPVA} (0;0,0)	114.6	60.9	111.3	119.4	111.0	61.9	61.2	88.3	56.3	55.9
β_{zzz} (0;0,0)	260.8	207.1	256.7	264.8	256.4	207.3	206.6	233.9	202.7	202.3
β_{zzz}^{nr} $(-\omega;\omega,0)_{\omega\to\infty}$	11.1									
β_{zzz}^{c-ZPVA} $(-\omega;\omega,0)_{\omega\to\infty}$	1.4	0.5	3.7	3.6	3.6	2.0	1.9	2.5	0.8	0.7
β_{zzz} $(-\omega;\omega,0)_{\omega\to\infty}$	43.6	42.7	45.1	45.0	45.0	43.4	43.3	44.1	43.2	43.1

[a]All computations were done at the MP2/POL level. Previously published data are compared with results obtained using the 1D relaxed, 1+5D HADA, 1+5D cHAC, 2D rigid, 2+4D HADA, and 2+4D cHAC quantum nuclear models (See sections 2A and 2B for definition of the various models). All quantities are in au. [b]Data taken from ref 9b. [c]Data taken from ref 2d. [d]Values obtained using a 6D quartic normal mode expansion of the PES and a FVCI wave function. [e]Values obtained using a 6D sextic normal mode expansion of the PES and a FVCI wave function. [f]Values obtained using a 1D relaxed PES, a symmetrized inversion curvilinear coordinate ($\theta = 1/3(\theta_1 + \theta_2 + \theta_3)$), and an exact numerical vibrational wave function. [g]Values obtained using a 1D relaxed PES, a symmetric inversion coordinate defined by displacement of the N atom perpendicular to the plane defined by the three hydrogen atoms, and an exact numerical vibrational wave function.

barrier of 117.94 cm^{-1} (or 6.2%) is much lower than the MP2/POL error of 347.67 cm^{-1} (or 18.5%). Moreover, the equilibrium geometries at the MP2/ATZ and higher *ab initio* levels are all very accurate with absolute errors in the N−H bond distance and H−N−H angles smaller than 0.004 Å and 0.2°, respectively. Using CCSD or CCSD(T) leads to a further decrease of the error in the inversion barrier; the largest error is, then, 49.12 cm^{-1} for CCSD(T)/ATZ and the smallest is 1.12 cm^{-1} for CCSD(T)/ACTZ. At this level of accuracy, as previously noted by one of us,[24a] the varying degree of agreement with experimental results is in part due to cancellation of errors caused by the combination of an incomplete basis set and the omission of higher-order electron correlation, as well as relativistic and adiabatic corrections. That is why, for instance, the error in the inversion barrier for CCSD/ATZ is less than for CCSD(T)/ATZ. Our computed CCSD(T) values are in very good agreement with those published by Halonen and co-workers[32b] and Lauvergnat and Nauts.[24a]

In Figure 4, we compare experimental values[41] of the first seven vibrational excited states ($E_{v=0} = 0.0$) for the inversion mode of ammonia with our theoretical results computed for six different quantum nuclear models using the PES obtained by several different *ab initio* electronic structure methods. This figure presents the mean absolute deviation (MAD) and maximum absolute deviation (MAXAD); the energy levels themselves are given as Supporting Information in Tables S1 and S2. Except in the case of the 1D relaxed quantum nuclear model, MP2/POL gives the worst results for all methods, as expected, since, as previously noted, the POL basis set was not designed to calculate the vibrational spectra. The improvement obtained when the MP2/ATZ PES is used indicates that the POL basis set is not as good a choice as ATZ.

The quantum nuclear models with two active coordinates give lower overall MAD and MAXAD values than the models with just one active coordinate with the improvement being larger for the HADA and cHAC methods. In fact, the differences between 2+4D HADA and 2+4D cHAC vibrational energy levels turn out to be very small. Indeed, the differences between 2+4D HADA and 2+4D cHAC vibrational energy levels are very small. Finally, for our best quantum nuclear model (i.e., 2+4D cHAC), the MP2/ATZ, CCSD/ATZ, CCSD/ACTZ, and CCSD(T)/ATZ methods all lead to similar MAD and MAXAD values, although the similar performance of MP2/ATZ and CCSD(T)/ATZ can only be explained by a cancellation of errors in the former case. The same general similarity of performance is obtained for the other quantum nuclear models as well.

Our CCSD(T)/ATZ 2D relaxed results are in excellent agreement with the results of Halonen and co-workers[32b] for the same method and an equivalent model. There is also very good agreement, again, between our CCSD(T)/ATZ 2+4D cHAC calculations and the CCSD(T)/ATZ 6D treatment of Thiel and co-workers,[42] which is based on the Hougen−Bunker−Johns formalism.[28b] Thus, our results present another example of the excellent performance obtained with the cHAC model. Thiel and co-workers also showed that if their 6D PES is determined using a CBS+ basis set, obtained by extrapolating aug-cc-pVXZ (X = T,Q,5) with relativistic effects included, then the MAXAD for the energy levels studied here is reduced to 4.5 cm^{-1}. Such calculations are, however, out of our range for computing the far more expensive vibrational NLO properties.

The inversion splitting of the vibrational ground state of ammonia is fully taken into account in the treatment of the vibrational NLO properties within our approach (see section 2C). In Figure 5, we compare experimental values[41] for inversion splitting in the ground state, as well as the three

Table 3. Electronic and Vibrational Contributions to the Diagonal Component of the Static and IOFA Dynamic Second Hyperpolarizabilities along the C_3 Symmetry Axis[a]

	6D normal modes		1D		ElVibRot					
	fourth-order[b,d]	sixth-order[b,e]	$\theta^{c,f}$	$z^{c,g}$	1D relaxed	1+5D HADA	1+5D cHAC	2D	2+4D HADA	2+4D cHAC
γ^{e}_{zzzz} (0;0,0,0)	7082									
γ^{nr}_{zzzz} (0;0,0,0)	7792									
γ^{ZPVA}_{zzzz} (0;0,0,0)	173	158	281	306	229	104	101	209	234	232
γ^{c-ZPVA}_{zzzz} (0;0,0,0)	25041	9504	22265	24036	22225	11366	11238	15442	10083	10025
γ_{zzzz} (0;0,0,0)	40088	24536	37420	39216	34651	26344	26213	30525	25191	25131
γ^{nr}_{zzzz} $(-\omega;\omega,0,0)_{\omega\to\infty}$	527									
γ^{c-ZPVA}_{zzzz} $(-\omega;\omega,0,0)_{\omega\to\infty}$	288	137	264	260	296	172	171	223	116	115
γ_{zzzz} $(-\omega;\omega,0,0)_{\omega\to\infty}$	8070	7904	8154	8175	8134	7885	7881	8041	7959	7956
γ^{nr}_{zzzz} $(-2\omega;\omega,\omega,0)_{\omega\to\infty}$	32									
γ^{c-ZPVA}_{zzzz} $(-2\omega;\omega,\omega,0)_{\omega\to\infty}$	11	19	−46	−48	−5	10	10	1	7	7
γ_{zzzz} $(-2\omega;\omega,\omega,0)_{\omega\to\infty}$	7298	7291	7349	7372	7338	7228	7225	7324	7355	7353

[a]The computations were done at the MP2/POL level. Previously published data are compared with results obtained using 1D relaxed, 1+5D HADA, 1+5D cHAC, 2D rigid, 2+4D HADA, and 2+4D cHAC quantum nuclear models (See sections 2A and 2B for definition of the various models). All quantities are in au. [b]Data taken from ref 9b. [c]Data taken from ref 2d. [d]Values obtained using a 6D quartic normal mode expansion of the PES and a FVCI wave function. [e]Values obtained using a 6D sextic normal mode expansion of the PES and a FVCI wave function. [f]Values obtained using a 1D relaxed PES, a symmetrized inversion curvilinear coordinate ($(\theta = 1/3(\theta_1 + \theta_2 + \theta_3))$), and an exact numerical vibrational wave function. [g]Values obtained using a 1D relaxed PES, a symmetric inversion coordinate defined by displacement of the N atom perpendicular to the plane defined by the three hydrogen atoms, and an exact numerical vibrational wave function.

lowest excited states, with our theoretical results. The MAD and MAXAD results are presented in the figure, whereas the numerical values are given as Supporting Information in Tables S3 and S4. As expected, most of the conclusions obtained for the individual levels are also valid for the inversion splittings: (i) the POL basis set leads to the worst results except for the 1D relaxed case; (ii) models with two active coordinates are better than those with one active coordinate; and (iii) the 2+4D HADA and 2+4D cHAC results are quite close to one another. In contrast to the individual levels, however, the inversion splittings for a single active coordinate always show improvement when a better quantum nuclear model is used. Thus, for example, the relaxed 1D MAD is cut in half by going to 1+5D HADA and by half again for 1+5D cHAC. It also turns out that the MAX and MAXAD for 1+5D cHAC are very similar to those for 2+4D cHAC. This makes the former model an excellent choice for computing the vibrational NLO properties of ammonia.

Because of compensating errors, the MP2/ATZ, CCSD/ATZ, CCSD/ACTZ, and CCSD(T)/ATZ PES lead to about equally good results for the inversion splittings. Taking into account the high computational cost of the vibrational (hyper)polarizability calculations, we chose CCSD/ACTZ as the *ab initio* method for determining the field-dependent energy and electronic properties surfaces required to evaluate the vibrational NLO properties by means of the finite field nuclear relaxation approach. Indeed, for the 2+4D cHAC quantum nuclear model, the CCSD/ACTZ PES reproduces the inversion splitting of the ground state better than all other possibilities considered here. Finally, for the inversion splittings (as in the case of the individual levels), our CCSD(T)/ATZ 2D and CCSD(T)/ATZ 2+4D cHAC results are in excellent agreement with, respectively, the CCSD(T)/ATZ 2D values of Halonen and co-workers[32b] and the CCSD(T)/ATZ 6D values of Thiel and co-workers.[42]

As discussed above, we have chosen CCSD/ACTZ as the preferred method for calculating the vibrational NLO properties presented in this paper. However, in Tables 2 and 3, we also report the vibrational (and electronic) contributions to the diagonal component of the (hyper)polarizabilities along the C_3 symmetry axis as computed by means of the MP2/POL method. This allows us to compare the results obtained here using our new approach with the vibrational (hyper)-polarizabilities that we obtained previously based either on a 1D relaxed model or a standard one-well treatment. The static electric fields in the finite field calculations were ±0.0004, ±0.0008, ±0.0016, ±0.0032, ±0.0064, and ±0.0128 au. We used the Romberg method triangle[43] to select the most accurate derivatives. In the second and third columns of Tables 2 and 3 are our previous results from the one-well treatment.[9b] Those calculations utilized a Taylor series expansion for both the PES and the electronic properties as a function of the normal coordinates ($\mathbf{Q}$). On one hand, the results obtained showed rapid convergence, with respect to the order in $\mathbf{Q}$, for the electronic properties. On the other hand, as can be seen in Tables 2 and 3, there was a big difference in the static vibrational (hyper)polarizabilities between the 6D quartic and 6D sextic normal mode expansions of the PES. For γ^{c-ZPVA}_{zzzz} (0;0,0,0), the most notable example of this divergence, the value obtained with the 6D quartic PES is close to 3 times larger than that obtained with the 6D sextic PES.

In a subsequent paper, we computed the same vibrational contributions using the 1D relaxed model.[2d] The results given in the fourth column of Tables 2 and 3 were obtained using the same active coordinate as in the present work,[2d] but with vibrational wave functions calculated by means of the exact numerical *shooting* method[44] rather than the ElVibRot code employed here. The data in the fifth column were obtained similarly except that the active coordinate was taken as the displacement between the plane defined by the three hydrogens and the N atom.[45] By comparing the static vibrational (hyper)polarizabilities in the second and third columns of Tables 2 and 3 with the 1D relaxation data presented in the next two columns, one might conclude (as we did) that the one-well results obtained with the 6D quartic PES are satisfactory, whereas those obtained with the sextic PES are

seriously flawed. However, it will be seen below that this is an erroneous conclusion to which we were led by an accidental compensation of errors for the 1D relaxed model.

In the last six columns of Tables 2 and 3, we show results obtained with our new approach for the six quantum nuclear models discussed in this paper. Considering the difference in the evaluation of the vibrational wave function (see above), there is good agreement between our new 1D relaxed data and our previous 1D relaxed results computed with the same coordinate. For these two cases, the values of the total electric property differ by less than 0.3%. However, the comparison of the 1D relaxed total (hyper)polarizabilities with the 2+4D cHAC results shows much larger differences. For the total static and IOFA dynamic hyperpolarizability the differences range from 4.4% to 26.7% for β and from 0.2% to 48.5% for γ. On the other hand, the 1+5D HADA quantum nuclear model leads to a dramatic improvement over the 1D-relaxed model. In the former case, the differences for the total static and IOFA dynamic hyperpolarizability with respect to the 2+4D cHAC values are reduced to 0.7−2.5% for β and 0.9−4.8% for γ. The 1+5D cHAC model is slightly better yet with differences of 0.5−2.1% for the total β and 0.9−4.3% for the total γ. The 2D relaxed model also improves on the 1D relaxed values, but the range of differences (with respect to 2+4D) is still large: 2.3−15.6% (0.4−21.5%) for β (γ). On the contrary, these differences are negligible for 2+4D HADA (i.e., less than 0.3%), showing an excellent convergence between the 2+4D HADA and 2+4D cHAC models. Finally, our previous one-well results based on a 6D sextic PES expansion agree very well with the reference 2+4D cHAC calculations (maximum differences for total properties less than 2.5%). Thus, the one-well 6D sextic PES expansion treatment could be a good methodology for calculating the vibrational NLO properties of single-well molecules, or multiwell molecules, with splitting equal to or less than ammonia, although it is difficult to be sure a priori what order expansion to employ. Nevertheless, for molecules with small barriers between equivalent minima, such as the HF dimer[46] and HOOH[47] (two equivalent minima with a potential energy barrier of 337 cm^{-1} and 357 cm^{-1}, respectively), the full dimensionality approaches presented here may be the only reliable way to obtain accurate vibrational NLO properties. For molecules with very small barriers, the only requirement to properly apply our approach is to check if the desired finite field calculations lie within the weak or strong field regime (or neither). Of course, the multiwell full dimensionality approach is reliable regardless of the barrier height. Thus, the convergence of the PES expansion is not a potential problem as it is in a one-well treatment. Moreover, one does not have to guess whether tunneling will or will not be important.

In Tables 4 and 5, we present the electronic and vibrational contributions to the diagonal component of the (hyper)-polarizabilities along the C_3 symmetry axis computed at the CCSD/ACTZ level using the 1D relaxed, 1+5D HADA, and 1+5D cHAC models. The MP2/POL results just discussed indicate that the 1+5D cHAC model will provide accurate values for the total vibrational NLO properties of ammonia. Some selected 2D relaxed values are also reported to confirm that the conclusions based on the MP2/POL method are followed at the CCSD/ACTZ level. As expected, we found that the MP2/POL and CCSD/ACTZ are completely consistent in that, for both methods, (i) the 1D relaxed total (hyper)-polarizabilities have large differences with respect to the 1+5D HADA model (maximum difference 65.3%); (ii) there is very good agreement between the 1+5D HADA and 1+5D cHAC properties (differences smaller than 1.0%); and (iii) the 2D-relaxed values lie in between the 1D-relaxed and 1+5D cHAC results.

Table 4. Electronic and Vibrational Contributions to the Dipole Moment and to the Diagonal Component of the Static Linear Polarizability, As Well As the Static and IOFA Dynamic First Hyperpolarizabilities, along the C_3 Symmetry Axis[a]

	1D relaxed	1+5D HADA	1+5D cHAC	2D
μ^{e}	−0.6006			
μ^{ZPVA}	0.0316	0.0208	0.0205	0.0280
μ	−0.5690	−0.5798	−0.5801	−0.5726
$\alpha_{zz}^{e}(0;0)$	14.61			
$\alpha_{zz}^{nr}(0;0)$	3.36			
$\alpha_{zz}^{ZPVA}(0;0)$	0.10	0.07	0.07	0.17
$\alpha_{zz}^{c-ZPVA}(0;0)$	1.56	0.93	0.92	1.54
$\alpha_{zz}(0;0)$	19.63	18.97	18.96	19.68
$\beta_{zzz}^{e}(0;0,0)$	24.0			
$\beta_{zzz}^{nr}(0;0,0)$	141.0			
$\beta_{zzz}^{ZPVA}(0;0,0)$	−1.1	−0.9	−0.9	−0.9
$\beta_{zzz}^{c-ZPVA}(0;0,0)$	255.4	138.6	136.5	188.9
$\beta_{zzz}(0;0,0)$	419.3	302.7	300.6	353.0
$\beta_{zzz}^{nr}(-\omega;\omega,0)_{\omega\to\infty}$	8.4			
$\beta_{zzz}^{c-ZPVA}(-\omega;\omega,0)_{\omega\to\infty}$	3.1	1.8	1.7	
$\beta_{zzz}(-\omega;\omega,0)_{\omega\to\infty}$	34.4	33.3	33.2	

[a]The computations were done at the CCSD/ACTZ level using the 1D relaxed, 1+5D HADA, 1+5D cHAC, and 2D rigid quantum nuclear models (see sections 2A and 2B for definition of the various models). All quantities are in au.

Table 5. Electronic and Vibrational Contributions to the Diagonal Component of the Static and IOFA Dynamic Second Hyperpolarizabilities along the C_3 Symmetry Axis[a]

	1D relaxed	1+5D HADA	1+5D cHAC
$\gamma_{zzzz}^{e}(0;0,0,0)$	4926		
$\gamma_{zzzz}^{nr}(0;0,0,0)$	11341		
$\gamma_{zzzz}^{ZPVA}(0;0,0,0)$	562	446	443
$\gamma_{zzzz}^{c-ZPVA}(0;0,0,0)$	55253	27292	26896
$\gamma_{zzzz}(0;0,0,0)$	72082	44005	43606
$\gamma_{zzzz}^{nr}(-\omega;\omega,0,0)_{\omega\to\infty}$	649		
$\gamma_{zzzz}^{c-ZPVA}(-\omega;\omega,0,0)_{\omega\to\infty}$	58	−9	−10
$\gamma zzzz(-\omega;\omega,0,0)_{\omega\to\infty}$	6195	6012	6008
$\gamma_{zzzz}^{nr}(-2\omega;\omega,\omega,0)_{\omega\to\infty}$	364		
$\gamma_{zzzz}^{c-ZPVA}(-2\omega;\omega,\omega,0)_{\omega\to\infty}$	−502	−464	−464
$\gamma_{zzzz}(-2\omega;\omega,\omega,0)_{\omega\to\infty}$	5350	5272	5269

[a]All computations were done at the CCSD/ACTZ level using the 1D relaxed, 1+5D HADA, 1+5D cHAC, and 2D rigid quantum nuclear models (see sections 2A and 2B for definition of the various models). All quantities are in au.

For the total dipole moment and total linear polarizability computed with the 1+5D cHAC model, the differences between the MP2/POL and CCSD/ACTZ calculations are quite small (less than 3.6% for μ and 1.7% for α). However, for the total first and second hyperpolarizabilities, these differences are between 30% and 39%. It is interesting that CCSD/ACTZ leads to an increase in the total static (hyper)polarizability with respect to MP2/POL, whereas the opposite is true for the dynamic properties. The static electronic contribution systematically decreases upon going from MP2/POL to CCSD/

dx.doi.org/10.1021/ct300805p | J. Chem. Theory Comput. 2013, 9, 520−532

ACTZ (maximum difference of 6.3% for α^{e}), whereas the nuclear relaxation contribution increases (maximum difference of 8.6% for static β^{nr}), with the only exception being $\beta^{nr}_{zzz}(-\omega;\omega,0)_{\omega\to\infty}$. Most of the increase in the CCSD/ACTZ static hyperpolarizabilites versus the corresponding MP2/POL values is due to the change in the dominant c-zpva contribution. On the contrary, for the IOFA dynamic hyperpolarizabilities the magnitude of the c-zpva contribution decreases upon going from MP2/POL to CCSD/ACTZ and its importance decreases as well. Finally, due to its small magnitude (see below), the variation of the zpva contribution caused by the change of the electronic structure method is negligible.

In agreement with previous published data,[2d,9b] our best results (i.e., CCSD/ACTZ with 1+5D cHAC model) confirm that nuclear motions play a key role in determining the electrical properties of ammonia. They make a contribution to the total static property value of 22.9%, 92.0%, and 88.7% for α, β, and γ, respectively. For the IOFA dynamic hyperpolarizabilites, their contribution is less important but still essential to reproducing the correct value of the nonlinear property. In the case of the Pockels effect (i.e., $\beta_{zzz}(-\omega;\omega,0)_{\omega\to\infty}$), for instance, the weight of the vibrational contributions is 30.4%. Whereas for static hyperpolarizabilities $P^{c\text{-}zpva}$ is similar to, or even larger than, P^{nr}, for IOFA dynamic hyperpolarizabilities, the former is always the smaller of the two. However, the P^{zpva} contribution itself is always quite small.

4. SUMMARY AND CONCLUSIONS

We have explored several full dimensionality approaches for calculating the vibrational contribution to nonlinear optical properties of molecules with large amplitude anharmonic vibrational modes using ammonia as a test case. Our treatment combines the FF-NR procedure, which treats low-order anharmonicity effects, with a generalization that, in principle, accounts for all remaining anharmonicity contributions. This generalization requires calculating the change in the zero point contribution to the vibrational energy and electrical properties associated with the geometry relaxation induced by a static electric field. For that purpose, we employed various quantum nuclear models, as implemented in Lauvergnat's ElVibRot code.[13] These models separate active and inactive coordinates. For the one or two active coordinates, the full vibrational potential is used. The remaining inactive modes are described by an approximate quadratic potential that depends on the instantaneous position of the active coordinates. Since curvilinear coordinates are used in both cases, a numerical, but exact, procedure is employed to obtain the kinetic energy operator.

As an illustrative example, we have computed the static and IOFA dynamic (hyper)polarizabilities of ammonia, which has a highly anharmonic double minimum inversion potential. The inversion motion is coupled harmonically (and anharmonically) to the symmetric N−H stretching motion. In order to properly account for inversion tunneling, generalized Van Vleck perturbation theory (GVV-PT) was utilized for the split pair of vibrational ground states. This is a general ingredient of our procedure that is needed whenever the contribution from tunneling between two or more potential wells is significant. For comparison, reduced dimensionality (1D and 2D) calculations were performed along with full dimensionality (1+5D and 2+4D) treatments. In the latter case, we considered two quantum nuclear models: (i) a single adiabatic channel (HADA) and (ii) coupled adiabatic channels (cHAC).

Initial calculations of the vibrational energy levels and inversion splittings, obtained with the various quantum nuclear models, were carried out for several basis sets and ab initio electron correlation methods. Taking accuracy and computational expense into account, it was found that the CCSD/ACTZ level best suited our purposes. We also learned that the 1+5D cHAC results for the inversion splittings were similar to those calculated for our best 2+4D cHAC model and for the 2+4D HADA model as well. The close agreement of the latter two suggested that a single uncoupled channel is sufficient to calculate the vibrational nonlinear optical properties.

Calculations of the nonlinear optical properties were done not only at the CCSD/ACTZ level but at the MP2/POL level as well in order to compare with previous results. Our 1D MP2/POL calculations show that the single-well (no tunneling) vibrational hyperpolarizabilities obtained with a 6D quartic PES agree quite well with those obtained from double-well 1D relaxed calculations. However, both sets of results differ substantially from those obtained with respect to the more accurate (HADA and cHAC) double-well quantum nuclear models that include coupling with the inactive modes. On the contrary, the 1D treatment with a single-well 6D sextic PES leads to vibrational hyperpolarizabilities that are in good agreement with these models. Thus, the single-well 6D sextic PES treatment could be satisfactory for calculating the vibrational hyperpolarizabilites of single-well molecules or of multiwell molecules with splittings less than or similar to those of ammonia, although it is difficult to know beforehand. In general, for multiwell molecules with larger splittings, n+mD cHAC or, possibly, HADA models should be utilized.

Our final CCSD/ACTZ results were obtained using the 1+5D cHAC model, as justified by the close agreement for vibrational energy levels and tunneling frequencies with the ultimate 2+4D cHAC model. For comparison, the 1D and 1+5D HADA models were employed as well. Although the 1D model is not satisfactory, the results for the HADA and cHAC models are in close agreement. In general, a good correlated electronic structure method and flexible basis set containing diffuse functions is required, along with full dimensionality, to accurately reproduce the vibrational nonlinear optical properties of ammonia. In line with our previous results, the CCSD/ACTZ 1+5D cHAC calculations indicate that the vibrational contributions to the static hyperpolarizabilities are larger than the corresponding electronic term. Although that is not true for the IOFA dynamic hyperpolarizabilities, the vibrational contribution remains important for most processes.

In the future, we want to consider molecules with very low barriers between equivalent minima, like the HF dimer[46] and HOOH,[47] for which tunneling will have an important role. The former has a more complex PES containing several coupled strongly anharmonic motions. In fact, it is already known that BKPT is nonconvergent for the HF dimer[4] and HOOH.[9a,48] In addition, DFT will be explored for greater efficiency in treating electron correlation.

■ ASSOCIATED CONTENT

Supporting Information

Tables showing the first seven excited states of the inversion mode of ammonia, their splittings, and their MAD and MAXD with respect to the experimental data computed using different electronic structure levels for the PES and 1D relaxed, 1+5D HADA, 1+5D cHAC, 2D, 2+4D HADA, and 2+4D cHAC

quantum nuclear models. This information is available free of charge via the Internet at http://pubs.acs.org/.

AUTHOR INFORMATION

Corresponding Author

*Phone: +30 210 7273894 (H.R.), +34 972418272 (J.M.L.). Fax: +30 210 7273831 (H.R.), +34 972418356 (J.M.L.). E-mail: hreis@eie.gr (H.R.), josepm.luis@udg.edu (J.M.L.).

Notes

The authors declare no competing financial interest.

ACKNOWLEDGMENTS

The following organizations are thanked for financial support: the European Union Seventh Framework Programme (FP7-REGPOT-2009-1, Grant N. 245866), the Spanish Ministerio de Ciencia e Innovación (MICINN, CTQ2011-23156/BQU), and the DIUE of the Generalitat de Catalunya (2009SGR637 and Xarxa de Referència en Química Teòrica i Computacional). M.G.-B. thanks the Spanish MEC for a doctoral fellowship no. AP2010-2517. Support for the research of M.S. was received through the ICREA Academia 2009 prize for excellence in research funded by the DIUE of the Generalitat de Catalunya. Financial support from MICINN and the FEDER fund (European Fund for Regional Development) was provided by grant UNGI08-4E-003.

REFERENCES

(1) (a) Kim, H. S.; Yoon, K. B. *J. Am. Chem. Soc.* **2012**, *134*, 2539−2542. (b) Zou, G.; Ye, N.; Huang, L.; Lin, X. *J. Am. Chem. Soc.* **2011**, *133*, 20001−20007. (c) Wang, S.; Ye, N. *J. Am. Chem. Soc.* **2011**, *133*, 11458−11461.

(2) (a) Ingamells, V. E.; Papadopoulos, M. G.; Sadlej, A. J. *J. Chem. Phys.* **2000**, *112*, 1645−1654. (b) Ingamells, V. E.; Papadopoulos, M. G.; Handy, N. C.; Willetts, A. *J. Chem. Phys.* **1998**, *109*, 1845−1859. (c) Loboda, O.; Zaleśny, R.; Avramopoulos, A.; Luis, J. M.; Kirtman, B.; Tagmatarchis, N.; Reis, H.; Papadopoulos, M. G. *J. Phys. Chem. A* **2009**, *113*, 1159−1170. (d) Luis, J. M.; Reis, H.; Papadopoulos, M.; Kirtman, B. *J. Chem. Phys.* **2009**, *131*, 034116. (e) Dutra, A. S.; Castro, M. A.; Fonseca, T. L.; Fileti, E. E.; Canuto, S. *J. Chem. Phys.* **2010**, *132*, 034307. (f) Zaleśny, R.; Bulik, I. W.; Bartkowiak, W.; Luis, J. M.; Avramopoulos, A.; Papadopoulos, M. G.; Krawczyk, P. *J. Chem. Phys.* **2010**, *133*, 244308. (g) Ferrabone, M.; Kirtman, B.; Rerat, M.; Orlando, R.; Dovesi, R. *Phys. Rev. B* **2011**, *83*, 235421. (h) Labidi, N. S.; Djebaili, A.; Rouina, I. *J. Saudi Chem. Soc.* **2011**, *15*, 29−37. (i) Naves, E. S.; Castro, M. A.; Fonseca, T. L. *J. Chem. Phys.* **2011**, *134*, 054315. (j) Reis, H.; Loboda, O.; Avramopoulos, A.; Papadopoulos, M. G.; Kirtman, B.; Luis, J. M.; Zaleśny, R. *J. Comput. Chem.* **2011**, *32*, 908−914. (k) Skwara, B.; Góra, R. W.; Zaleśny, R.; Lipkowski, P.; Bartkowiak, W.; Reis, H.; Papadopoulos, M. G.; Luis, J. M.; Kirtman, B. *J. Phys. Chem. A* **2011**, *115*, 10370−10381. (l) Torrent-Sucarrat, M.; Anglada, J. M.; Luis, J. M. *J. Chem. Theory Comput.* **2011**, *7*, 3935−3943. (m) Naves, E. S.; Castro, M. A.; Fonseca, T. L. *J. Chem. Phys.* **2012**, *136*, 014303.

(3) (a) Bishop, D. M.; Kirtman, B. *J. Chem. Phys.* **1991**, *95*, 2646−2658. (b) Bishop, D. M.; Kirtman, B. *J. Chem. Phys.* **1992**, *97*, 5255−5256. (c) Bishop, D. M.; Luis, J. M.; Kirtman, B. *J. Chem. Phys.* **1998**, *108*, 10013−10017.

(4) (a) Bishop, D. M.; Pipin, J.; Kirtman, B. *J. Chem. Phys.* **1995**, *102*, 6778−6786. (b) Eckart, U.; Sadlej, A. J. *Mol. Phys.* **2001**, *99*, 735−743.

(5) (a) Bishop, D. M.; Hasan, M.; Kirtman, B. *J. Chem. Phys.* **1995**, *103*, 4157−4159. (b) Luis, J. M.; Duran, M.; Andrés, J. L. *J. Chem. Phys.* **1997**, *107*, 1501−1512. (c) Kirtman, B.; Luis, J. M.; Bishop, D. M. *J. Chem. Phys.* **1998**, *108*, 10008−10012. (d) Luis, J. M.; Martí, J.; Duran, M.; Andrés, J. L.; Kirtman, B. *J. Chem. Phys.* **1998**, *108*, 4123−4130.

(6) (a) Bishop, D. M.; Dalskov, E. K. *J. Chem. Phys.* **1996**, *104*, 1004−1011. (b) Quinet, O.; Champagne, B. *J. Chem. Phys.* **1998**, *109*, 10594−10602. (c) Luis, J. M.; Duran, M.; Kirtman, B. *J. Chem. Phys.* **2001**, *115*, 4473−4483.

(7) Bishop, D. M.; Kirtman, B. *J. Chem. Phys.* **1998**, *109*, 9674−9676.

(8) (a) Luis, J. M.; Champagne, B.; Kirtman, B. *Int. J. Quantum Chem.* **2000**, *80*, 471−479. (b) Luis, J. M.; Duran, M.; Champagne, B.; Kirtman, B. *J. Chem. Phys.* **2000**, *113*, 5203−5213.

(9) (a) Torrent-Sucarrat, M.; Luis, J. M.; Kirtman, B. *J. Chem. Phys.* **2005**, *122*, 204108. (b) Luis, J. M.; Torrent-Sucarrat, M.; Christiansen, O.; Kirtman, B. *J. Chem. Phys.* **2007**, *127*, 084118.

(10) (a) Christiansen, O. *J. Chem. Phys.* **2005**, *122*, 194105. (b) Christiansen, O.; Kongsted, J.; Paterson, M. J.; Luis, J. M. *J. Chem. Phys.* **2006**, *125*, 214309. (c) Hansen, M. B.; Christiansen, O.; Hattig, C. *J. Chem. Phys.* **2009**, *131*, 154101. (d) Seidler, P.; Sparta, M.; Christiansen, O. *J. Chem. Phys.* **2011**, *134*, 054119. (e) Hansen, M. B.; Christiansen, O. *J. Chem. Phys.* **2011**, *135*, 154107.

(11) Kirtman, B.; Luis, J. M. *Int. J. Quantum Chem.* **2011**, *111*, 839−847.

(12) Lauvergnat, D.; Nauts, A. *J. Chem. Phys.* **2002**, *116*, 8560−8570.

(13) Lauvergnat, D.; Nauts, A. *Phys. Chem. Chem. Phys.* **2010**, *12*, 8405−8412.

(14) Bowman, J. M.; Carrington, T.; Meyer, H. D. *Mol. Phys.* **2008**, *106*, 2145−2182.

(15) (a) Carter, S.; Bowman, J. M.; Handy, N. C. *Theor. Chem. Acc.* **1998**, *100*, 191−198. (b) Chaban, G. M.; Jung, J. O.; Gerber, R. B. *J. Chem. Phys.* **1999**, *111*, 1823−1829. (c) Rauhut, G. *J. Chem. Phys.* **2004**, *121*, 9313−9322. (d) Benoit, D. M. *J. Chem. Phys.* **2006**, *125*, 244110. (e) Cassam-Chenai, P.; Lievin, J. *J. Comput. Chem.* **2006**, *27*, 627−640.

(16) Mátyus, E.; Czakó, G.; Császár, A. G. *J. Chem. Phys.* **2009**, *130*, 134112.

(17) Yurchenko, S. N.; Thiel, W.; Jensen, P. *J. Mol. Spectrosc.* **2007**, *245*, 126−140.

(18) von Horsten, H. F.; Rauhut, G.; Hartke, B. *J. Phys. Chem. A* **2006**, *110*, 13014−13021.

(19) Scribano, Y.; Lauvergnat, D. M.; Benoit, D. M. *J. Chem. Phys.* **2010**, *133*, 094103.

(20) Beck, M. H.; Jäckle, A.; Worth, G. A.; Meyer, H. D. *Phys. Rep.* **2000**, *324*, 1−105.

(21) Schröeder, M.; Gatti, F.; Meyer, H.-D. *J. Chem. Phys.* **2011**, *134*, 234307.

(22) (a) Baltagi, F.; Bauder, A.; Ueda, T.; Gunthard, H. H.; Henrici, P. *Mol. Phys.* **1972**, *24*, 945−968. (b) Chapuisat, X.; Brunet, J. P.; Nauts, A. *Chem. Phys. Lett.* **1987**, *136*, 153−163. (c) Gatti, F.; Iung, C. *Phys. Rep.* **2009**, *484*, 1−69.

(23) (a) Rush, D. J.; Wiberg, K. B. *J. Phys. Chem. A* **1997**, *101*, 3143−3151. (b) Gatti, F.; Justum, Y.; Menou, M.; Nauts, A.; Chapuisat, X. *J. Mol. Spectrosc.* **1997**, *181*, 403−423.

(24) (a) Lauvergnat, D.; Nauts, A. *Chem. Phys.* **2004**, *305*, 105−113. (b) Blasco, S.; Lauvergnat, D. *Chem. Phys. Lett.* **2003**, *373*, 344−349.

(25) (a) Light, J. C.; Bačić, Z. *J. Chem. Phys.* **1987**, *87*, 4008−4019. (b) Fehrensen, B.; Luckhaus, D.; Quack, M. *Chem. Phys. Lett.* **1999**, *300*, 312−320.

(26) Miller, W. H.; Handy, N. C.; Adams, J. E. *J. Chem. Phys.* **1980**, *72*, 99−112.

(27) Carrington, T.; Miller, W. H. *J. Chem. Phys.* **1984**, *81*, 3942−3950.

(28) (a) Meyer, R.; Gunthard, H. H. *J. Chem. Phys.* **1969**, *50*, 353−365. (b) Hougen, J. T.; Bunker, P. R.; Johns, J. W. C. *J. Mol. Spectrosc.* **1970**, *34*, 136−172. (c) Bowman, J. M.; Gazdy, B. *J. Chem. Phys.* **1990**, *93*, 1774−1784.

(29) (a) Smeyers, Y. G.; Melendez, F. J.; Senent, M. L. *J. Chem. Phys.* **1997**, *106*, 1709−1717. (b) Muñoz-Caro, C.; Niño, A. *Quant. Chem. Program Exch. Bull.* **1993**, *13*, 4. (c) Senent, M. L. *Chem. Phys. Lett.* **1998**, *296*, 299−306.

(30) (a) Laane, J.; Harthcock, M. A.; Killough, P. M.; Bauman, L. E.; Cooke, J. M. *J. Mol. Spectrosc.* **1982**, *91*, 286−299. (b) Harthcock, M. A.; Laane, J. *J. Mol. Spectrosc.* **1982**, *91*, 300−324.

(31) Chapuisat, X.; Belafhal, A.; Nauts, A. *J. Mol. Spectrosc.* **1991**, *149*, 274−304.
(32) (a) Handy, N. C.; Carter, S.; Colwell, S. M. *Mol. Phys.* **1999**, *96*, 477−491. (b) Pesonen, J.; Miani, A.; Halonen, L. *J. Chem. Phys.* **2001**, *115*, 1243−1250. (c) Gatti, F.; Iung, C.; Leforestier, C.; Chapuisat, X. *J. Chem. Phys.* **1999**, *111*, 7236−7243. (d) Martin, J. M. L.; Lee, T. J.; Taylor, P. R. *J. Chem. Phys.* **1992**, *97*, 8361−8371.
(33) Moller, C.; Plesset, M. S. *Phys. Rev.* **1934**, *46*, 0618−0622.
(34) (a) Cizek, J. *Advances in Chemical Physics*; Wiley Interscience: New York, 1969; Vol. *14*, pp 35−90; (b) Purvis, G. D.; Bartlett, R. J. *J. Chem. Phys.* **1982**, *76*, 1910−1918.
(35) Watts, J. D.; Gauss, J.; Bartlett, R. J. *J. Chem. Phys.* **1993**, *98*, 8718−8733.
(36) Sadlej, A. J. *Collect. Czech. Chem. Commun.* **1988**, *53*, 1995−2016.
(37) (a) Dunning, T. H. *J. Chem. Phys.* **1989**, *90*, 1007−1023. (b) Kendall, R. A.; Dunning, T. H.; Harrison, R. J. *J. Chem. Phys.* **1992**, *96*, 6796−6806.
(38) Woon, D. E.; Dunning, T. H. *J. Chem. Phys.* **1995**, *103*, 4572−4585.
(39) Frisch, M. J.; Trucks, G. W.; Schlegel, H. B.; Scuseria, G. E.; Robb, M. A.; Cheeseman, J. R.; Scalmani, G.; Barone, V.; Mennucci, B.; Petersson, G. A.; Nakatsuji, H.; Caricato, M.; Li, X.; Hratchian, H. P.; Izmaylov, A. F.; Bloino, J.; Zheng, G.; Sonnenberg, J. L.; Hada, M.; Ehara, M.; Toyota, K.; Fukuda, R.; Hasegawa, J.; Ishida, M.; Nakajima, T.; Honda, Y.; Kitao, O.; Nakai, H.; Vreven, T.; Montgomery, J. A., Jr.; Peralta, J. E.; Ogliaro, F.; Bearpark, M.; Heyd, J. J.; Brothers, E.; Kudin, K. N.; Staroverov, V. N.; Kobayashi, R.; Normand, J.; Raghavachari, K.; Rendell, A.; Burant, J. C.; Iyengar, S. S.; Tomasi, J.; Cossi, M.; Rega, N.; Millam, J. M.; Klene, M.; Knox, J. E.; Cross, J. B.; Bakken, V.; Adamo, C.; Jaramillo, J.; Gomperts, R.; Stratmann, R. E.; Yazyev, O.; Austin, A. J.; Cammi, R.; Pomelli, C.; Ochterski, J. W.; Martin, R. L.; Morokuma, K.; Zakrzewski, V. G.; Voth, G. A.; Salvador, P.; Dannenberg, J. J.; Dapprich, S.; Daniels, A. D.; Farkas, Ö.; Foresman, J. B.; Ortiz, J. V.; Cioslowski, J.; Fox, D. J. *Gaussian 09*, revision C.01, revision C.01; Gaussian, Inc.: Wallingford. CT, 2009.
(40) (a) Špirko, V.; Kraemer, W. P. *J. Mol. Spectrosc.* **1989**, *133*, 331−344. (b) *Landolt-Börnstein: Numerical Data and Functional Relationships in Science and Technology II*; Springer: New York, 1976.
(41) Špirko, V. *J. Mol. Spectrosc.* **1983**, *101*, 30−47.
(42) Yurchenko, S. N.; Zheng, J. G.; Lin, H.; Jensen, P.; Thiel, W. *J. Chem. Phys.* **2005**, *123*, 104317.
(43) Davis, P. J.; ; Rabinowitz, P. In *Numerical Integration*, Blaisdell: London, 1967; p 166.
(44) Press, W. H.; Teukolsky, S. A.; Vetterling, W. T.; Flannery, B. P. In *Numerical Recipes*; Cambridge University Press: Cambridge, U. K., 1992.
(45) Aquino, N.; Campoy, G.; Yee-Madeira, H. *Chem. Phys. Lett.* **1998**, *296*, 111−116.
(46) Klopper, W.; Quack, M.; Suhm, M. A. *J. Chem. Phys.* **1998**, *108*, 10096−10115.
(47) Lee, J. S. *Chem. Phys. Lett.* **2002**, *359*, 440−445.
(48) Santiago, E.; Castro, M. A.; Fonseca, T. L.; Mukherjee, P. K. *J. Chem. Phys.* **2008**, *128*, 064310.